

# Crystallization and Melting Behaviors of Poly(aryletheretherketone) (PEEK) on Origin of Double Melting Peaks

C. BAS,\* P. BATTESTI, and N. D. ALBÉROLA

ESIGEC, Université de Savoie, Laboratoire Matériaux Composites, Campus scientifique, bâtiment "Le Chablais," 73376 Le Bourget-du-Lac, France

## SYNOPSIS

The crystallization and melting behaviors of poly(aryletheretherketone) (PEEK) films were investigated, using differential scanning calorimetry and metallurgy concepts. The shape of the time-temperature-transformation (TTT) diagram, established for PEEK, results from both nucleation and growth phenomena. The double melting behavior exhibited by isothermally crystallized PEEK samples are discussed through the TTT diagram and the influence of the thermal history in the molten state. The upper melting peak arises first and the lower melting peak is developed later. The location of such a second endotherm is shifted toward the higher temperature with increasing either the crystallization temperature or the annealing time while the location of the upper melting peak seems to be unchanged. The double melting behavior is related to a bimodal distribution in size and/or perfection of lamellae developed in a two-step crystallization. With increasing temperature and/or annealing time in the molten state, the pattern of the endothermic curves is modified. The observed changes are discussed through two origins: the progressive disappearance of remnants of the former crystals and a thermal degradation leading to a cross-linking of the polymer. © 1994 John Wiley & Sons, Inc.

## INTRODUCTION

Mechanical behavior of poly(aryletheretherketone) PEEK depends on the microstructure. The isothermal and nonisothermal crystallizations of PEEK and the resulting microstructure have been studied extensively by using various methods such as differential scanning calorimetry (DSC), infrared (IR) spectroscopy, optical microscopy, wide angle X-ray scattering (WAXS), small angle X-ray scattering (SAXS), and electron microscopy.<sup>1-16</sup>

Isothermally crystallized samples at high and low temperatures both show two melting peaks for crystallization times that are large enough. Such complex melting behavior has been shown by many authors for many polymers: PEEK,<sup>15-22</sup> poly(etheretherketoneketone),<sup>23</sup> poly(phenylene sulfide),<sup>24,25</sup> polyethylene,<sup>26-28</sup> polyimide,<sup>29</sup> and polyethylene terephthalate.<sup>30</sup> The explanations for the complex

melting behavior of PEEK can be grouped into the three following categories.

**Category 1.** The double melting behavior of PEEK results from melting and recrystallization phenomena of one initial crystal morphology developed during the prior crystallization history.<sup>17-20</sup> The first endotherm located at the lower temperature is related to the melting trace of the crystallites formed during isothermal crystallization. The melting of such crystallites would be immediately followed by the recrystallization process leading to more perfect and/or thicker lamellae. The crystallization exotherm related to such a phenomenon would be masked by the presence of melting peaks. The more stable lamellae so-formed, melt at higher temperatures. According to Blundell,<sup>17</sup> the decrease in the position of the main peak with increasing heating rate, seen as a result of the dynamics of the recrystallization phenomenon, supports this hypothesis. But, according to Basset et al.,<sup>16</sup> because variations in peak size are modest versus heating rate, even at the highest rate (80°C/min), this shows no evidence for a simple untransformed melt-

\* To whom correspondence should be addressed.

ing peak. Reorganization would have to be fast compared with the highest scanning rate to retain the double peaked character than almost undiminished state. Such an origin in the double melting behavior was also proposed for polyethylene<sup>28</sup> and for polyethylene terephthalate.<sup>30</sup>

**Category 2.** The double melting endotherms in PEEK could be due to the presence of two initial distinct populations of crystalline lamellae.<sup>15,16,21,22</sup> Transmission electron microscopy observations showing two crystal populations with different lamellae thicknesses support such an interpretation.<sup>16,22</sup>

According to a number of authors,<sup>15,16,21,22</sup> the upper endothermic peak is related to the melting of the main crystal population first developed on isothermal crystallization, whereas the lower endothermic peak could be due to the melting of the smaller lamellae formed in the intermediate spaces.<sup>15,16,21,22</sup> The formation of two crystallite populations would result from two populations of molecules that can phase separate in the melt.<sup>22</sup> Such an interpretation was also proposed for the double melting behavior of other polymers<sup>26,27,29,31</sup> such as polyethylene<sup>26,27</sup> and supported by transmission electron microscopy observations.<sup>32</sup>

**Category 3.** According to Marand and Prasad,<sup>33</sup> the double melting behavior exhibited by PEEK for crystallization temperatures above 300°C could be due to the formation of two morphologies, spherulitic and crystal-aggregate-like structures. For crystallization temperatures below 300°C, a single morphology, that is, spherulitic structure was observed by these authors. However, this does not explain the occurrence of a second melting peak for crystallization temperatures below 300°C.

Another hypothesis, consistent with category 2, was provided by Alberola<sup>26</sup> to interpret the origin of the double population of lamellae in polyethylene. Thus, isothermally crystallized samples of polyethylene at temperatures above the "nose" of the TTT diagram and then quenched at room temperature exhibit two melting endotherms related to two distinct crystallite populations. At low supercooling, the rate of crystallization growth is higher than the nucleation rate. So the primary nuclei resulting from residues of the previous crystalline organization could grow and large lamellae are formed. On cooling to room temperature and again on heating for recording the melting endotherm, the sample "crosses" the crystallization zone. Thus, secondary nuclei appeared from the remaining uncrystallized fraction and small lamellae are formed. The amount of such crystallites depends on the remaining uncrystallized

material, that is, the annealing time at the crystallization temperature. Then, two populations of crystallites showing different thicknesses can be formed.

This work, based on Albérola's concept,<sup>26</sup> deals with the origin of the double melting behavior displayed by PEEK. For this aim, the TTT curves are established from isothermal crystallization kinetics and the influence of the thermal history will be discussed.

## EXPERIMENTAL

### Materials

The polymer used in this study was PEEK Stabar K200 supplied by ICI (U.K.) in the form of amorphous sheets with thickness of about 250  $\mu\text{m}$ . The average molecular weights  $M_w$  and  $M_n$  are given between 95,000–120,000 g/mol and 35,000–50,000 g/mol, respectively.

### DSC Experiments

DSC experiments were carried out over the temperature range from 50 to 400°C by using a Perkin-Elmer DSC-7 instrument purged with helium gas with chilled liquid nitrogen. Thermograms were calibrated by scanning melting point substances, indium and zinc, at the heating rate at which DSC traces of analyzed samples were recorded. Baselines were determined by running an empty can at the given scan rate of the analyzed samples giving a curve subtracted from the specimen thermograms.

Isothermal crystallization kinetics were performed for various supercooling degrees. For crystallization kinetics carried out at low supercooling (melt crystallization), the sample was first heated to 400°C for 5 min, which seems to be the optimal molten state conditions according many authors.<sup>4,34</sup> Then, the sample was quickly quenched down to the crystallization temperature range 290–325°C. Because the material could crystallize on cooling at temperatures below 290°C, the crystallization domain at high supercooling degree (cold crystallization) is determined from the glassy state. Thus, the samples were heated from room temperature at a heating rate of 200°C/min to the crystallization temperatures of 155–175°C. Above 175°C, the heating rate is not quick enough to avoid the occurrence of the crystallization during this increase in temperature.

Melting endotherms reported in this study are recorded at only one heating rate of 100°C/min in

order to minimize the reorganization phenomena which could occur on heating.<sup>5,20</sup>

### Fourier Transform Infrared Spectroscopy Analysis (FTIR)

The FTIR measurements were performed on a Perkin-Elmer 2000 Fourier Transform Infrared Spectrometer with a resolution of  $1\text{ cm}^{-1}$ . For each spectrum, 64 scans were accumulated. PEEK films with a thickness of about  $250\text{ }\mu\text{m}$  were used for FTIR measurements in transmission work. The high sample thickness for FTIR investigations displays both an advantage and a disadvantage. The disadvantage is that the strongest bands of PEEK, bands lower than  $1680\text{ cm}^{-1}$ , show complete absorption and then do not provide information. The advantage is that possible new weak bands arising from the degradation can be more easily detected. In order to analyze the strongest absorption bands displayed by PEEK, such an analysis was completed by FTIR experiments performed on PEEK powder in KBr pellets.

## RESULTS AND DISCUSSION

### Isothermal Crystallization Behavior: TTT Diagram

From the isothermal crystallization kinetics determined from both the molten and amorphous states, TTT diagram of PEEK was established as follow.

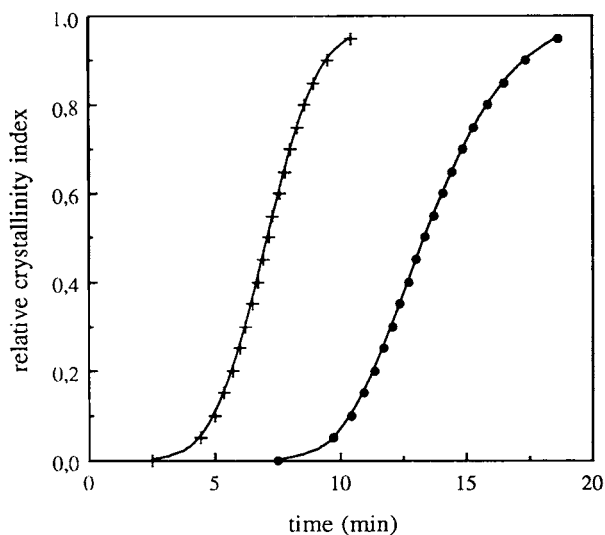


**Figure 1** Changes in the relative crystallinity indexes with the annealing time at different crystallization temperatures: ( + ) at  $160^{\circ}\text{C}$  from the amorphous state and ( ● ) at  $320^{\circ}\text{C}$  from the melt.

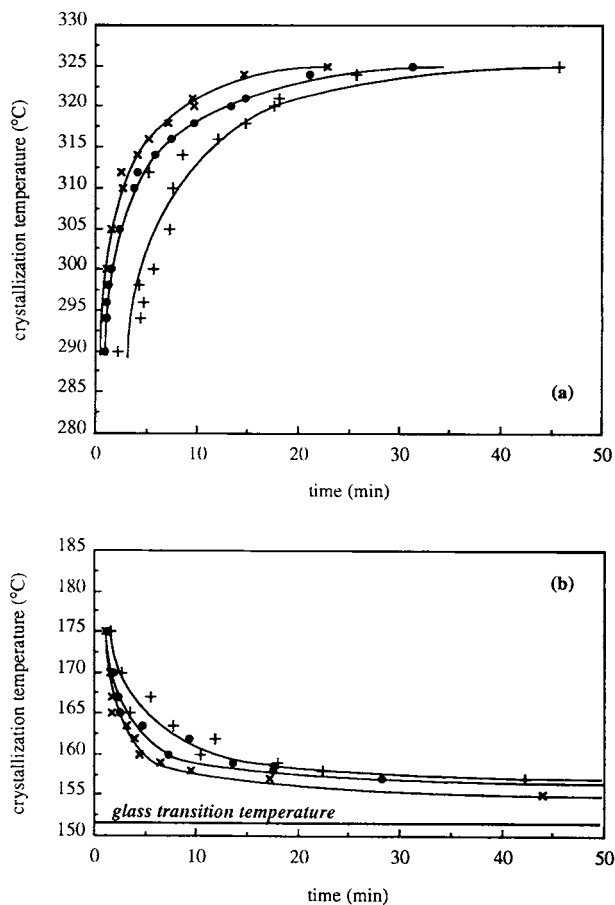


**Figure 2** Time-temperature-transformation (TTT) diagram (a) from the molten state and (b) from the glassy state for different relative crystallinity ratios: ( x ) 5%; ( ● ) 50%; ( + ) 95%.

From the exothermic peak recorded for one temperature, the relative crystallinity ratio ( $X_{cr}$ ) can be determined through the following relationship:

$$X_{cr}(T, t) = \frac{\Delta H_T(t)}{\Delta H_T(\infty)}$$

where  $\Delta H_T(\infty)$  is the total area under the crystallization exotherm at the crystallization temperature,  $T$ , and  $\Delta H_T(t)$  is the partial area for an annealing time  $t$  at the same crystallization temperature,  $T$ . Figure 1 shows the variations of the relative crystallinity index ( $X_{cr}$ ) versus time. The sigmoidal shape of the crystallization kinetics results from a two-step mechanism, nucleation and then growth phenomena.

By plotting the curves representing equal relative amount of crystallized material, the TTT diagram can be drawn for the analyzed crystallization temperature range (Fig. 2). The shape of the TTT

curves shows that the overall crystallization, including both nucleation and growth phenomena, locates in a wide temperature range. Because nucleation and growth rates evolve in opposite ways on varying the crystallization temperature, the overall crystallization rate passes through a maximum located between 175 and 290°C. Thus, above the nose of the TTT curves, the rate of crystallization growth is higher than the nucleation rate. At low temperatures, below the nose of the TTT diagram, nucleation is favored to the detriment of the growth.

### Melting Behavior of Isothermally Crystallized Samples

#### *Comparison Between Melting Behaviors after Isothermal Crystallizations at Low and High Supercoolings*

After isothermal crystallizations either at 310 or 160°C for 30 min, respectively, PEEK films were heated at 100°C/min after being cooled to room temperature (Fig. 3).

Whatever the crystallization conditions are, samples exhibit a double melting behavior. The sample crystallized at 310°C for 30 min exhibits two well-defined melting endotherms located at about 331 and 346°C, respectively. The sample isothermally crystallized at 160°C for 30 min also shows

two melting endotherms centered at 184 and 344°C, respectively. Moreover, both thermograms displayed by isothermally crystallized samples at 160 and 310°C exhibit a change in the baseline located at about 150°C, which is related to the glass transition. For the isothermally crystallized sample at 160°C, an exothermic transition can be distinguished at about 200°C resulting from the anisothermal crystallization phenomenon.

Various hypothesis have been proposed to interpret such a complex melting behavior. But, all studies agree on one point: crystals that melt at the lower temperature are those formed during the isothermal crystallization. Then, according to the Gibbs-Thomson relation, one could conclude that lamellae formed on cold crystallization are thinner and/or less perfect than those crystallized from the melt. This could result from hindrance in the growth rate crystallization when the crystallization temperature decreases. Such a conclusion agrees with the origin of the TTT diagram shape.

#### *Influence of Annealing Time at Crystallization Temperature on Double Melting Behavior*

*Isothermally Crystallized Samples at Low Supercooling Degree.* Figure 4 shows the melting endotherms recorded at a heating rate of 100°C/min after

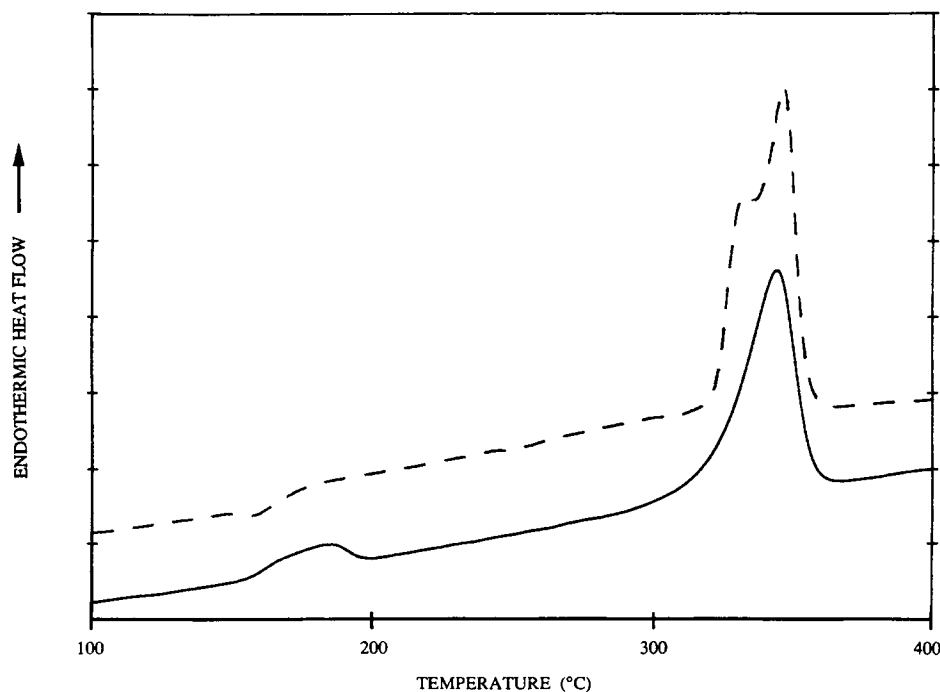


**Figure 3** Thermograms recorded at 100°C/min of isothermal crystallized PEEK for 30 min (—) at 160°C or (---) at 310°C.

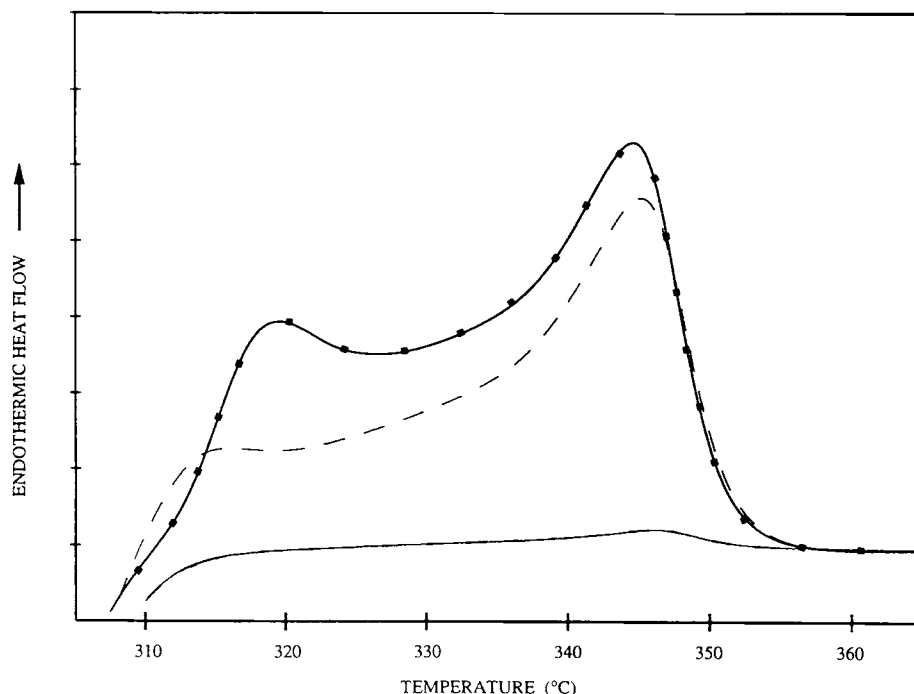


**Figure 4** Melting endotherms recorded at 100°C/min of isothermally crystallized samples at 300°C for: (—) a few seconds; (---) 1 min; (—■—■) 60 min.

isothermal crystallization at 300°C for various annealing times. The sample held for a few seconds at this temperature exhibits a single melting peak located at about 345°C whereas the specimen crystallized at this temperature for 1 min shows two melting endotherms. Whatever the annealing time, the upper melting peak locates at the same temperature.

With increasing crystallization time, the lower temperature melting peak shifted toward the higher temperatures and the area under the endothermic peaks rises, that is, the crystallinity ratio increases. Melting enthalpy values of the crystallized samples at 300°C for various annealing times are reported in Table I.

Figure 5 shows melting thermograms recorded at a heating rate of 100°C/min after isothermal crystallization at 320°C for various annealing times. For an annealing time of 1 h, it was observed that there were two well-defined melting peaks located at about 342 and 355°C; melting peaks exhibited by the sample crystallized at 300°C for the same annealing time are located at 319 and 344°C, respectively. This result is in agreement with the increase in crystallization growth rate when raising the crystallization temperature, as previously suggested.

Moreover, with increasing annealing time at 320°C from 1 h up to 36 h, both melting peaks shifted

toward higher temperatures. Thus, the lower temperature peak exhibited by the sample crystallized at 320°C for 36 h appears as a shoulder of the main upper melting peak. With increasing annealing time,

**Table I** Melting Enthalpy Values of Isothermally Crystallized Samples

Crystallization Time	Melting Enthalpy (J/g)
Crystallization at 300°C	
Few seconds	+1.0 ± 0.5
1 min	+36 ± 1
5 min	+41 ± 1
20 min	+43 ± 1
60 min	+46 ± 1
Crystallization at 320°C	
1 h	+43 ± 1
6 h	+49 ± 1
12 h	+50 ± 1
36 h	+52 ± 1
Crystallization at 160°C	
30 min	+28 ± 2
120 min	+31 ± 2

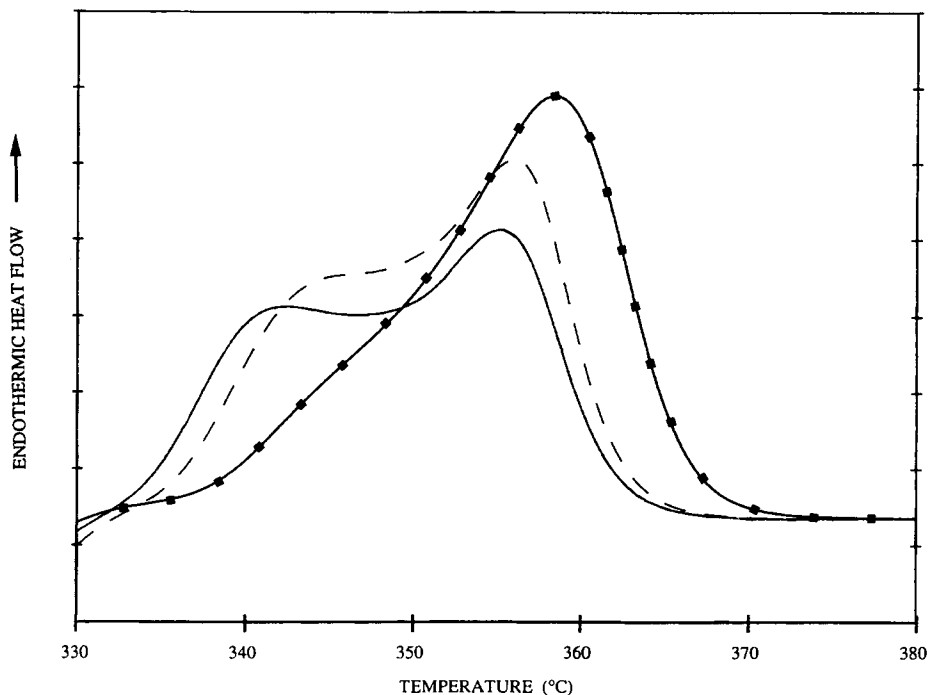


**Figure 5** Melting endotherms recorded at 100°C/min of isothermally crystallized samples at 320°C for: (—) 1 h; (---) 6 h; (—■—■) 36 h.

the melting enthalpy increases, that is, the crystalline amount increased (Table I).

According to the TTT diagram (Fig. 2), no further significant crystallization could occur for crystallization times up to 5 and 20 min at 300 and 320°C, respectively. But, some changes both in the pattern of the melting endotherm and in the crystallinity indexes are shown for annealing times larger than 5 and 20 min. This could be interpreted according to the two assumptions: perfection degree of crystallites is increased on annealing at the crystallization temperature; on recording the melting endotherm, the crystallization domain is crossed and then the formed lamellae could undergo some annealing.

*Isothermally Crystallized Samples at High Supercooling Degree.* Figure 6 shows melting endotherms recorded at a heating rate of 100°C/min after isothermal crystallization at 160°C for 30 and 120 min, respectively, and, then, quenched to 50°C.

Samples crystallized at 160°C for 30 and 120 min both exhibit two melting peaks. With increased holding time, the lower temperature endothermic peak was shifted from 184 and 191°C and the main upper peak was increased from 344 to 347°C. But no significant change in the melting enthalpy value was detected between these two holding times at 160°C (Table I).

### Conclusions on Origin of Double Melting Behavior

All these results suggest the following conclusion. Isothermally crystallized samples for high and low supercooling degrees both exhibit two stages of crystallization. The first step, which occurs quickly, leads to the large upper melting peak (Fig. 4). As a matter of fact, a few seconds at 300°C are sufficient to form crystallites that melt at about 345°C. The lower melting peak can be related to the melting of crystallites developed later during the annealing time. On heating scan, the thinner lamellae and/or the less perfect crystallites rapidly melt whereas the thickest lamellae and/or more perfect crystallites grow because the crystallization domain (see TTT diagram, Fig. 2) is crossed during this increase in temperature. The decrease in temperature location of the upper melting peak with increasing heating rate shown by others<sup>16,17,20</sup> is consistent with such an explanation. Accordingly, for high heating rates, the TTT curves are crossed for a weaker fraction of crystallized phase. Then, further crystallization or recrystallization is hindered and the ability of the lamellae to grow during the scan is reduced. This leads to a shift toward lower temperatures of the melting peak. Moreover, the location of the lower temperature melting endotherm appears to be strongly dependent on the supercooling degree (Fig.

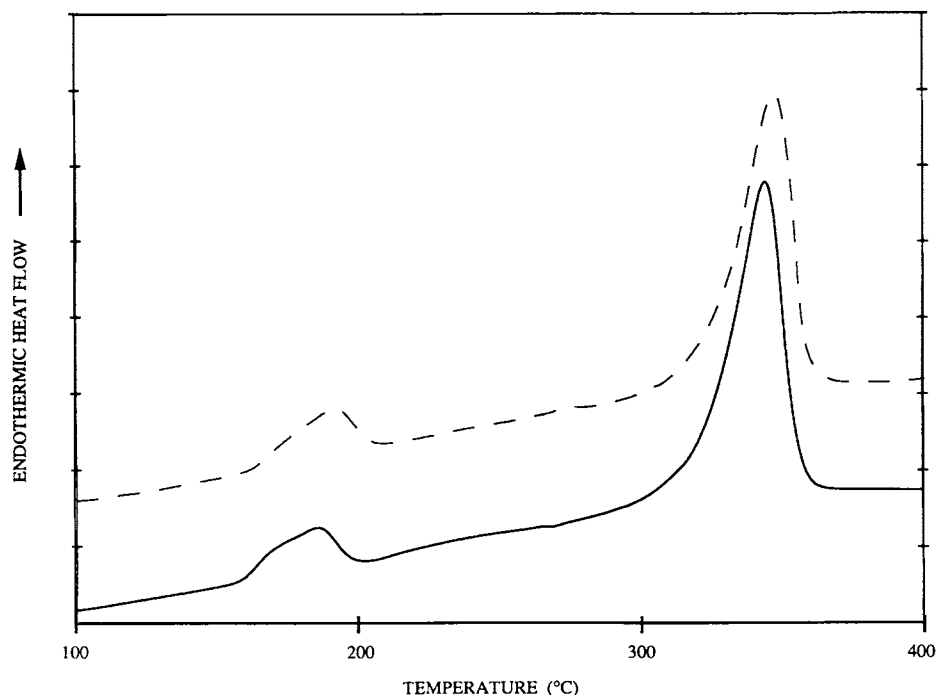


**Figure 6** Melting endotherms recorded at  $100^{\circ}\text{C}/\text{min}$  of isothermally crystallized samples at  $160^{\circ}\text{C}$  for: (—) 30 min and (---) 120 min.

3), that is, the predominance of nucleation or growth processes, whereas the position in the upper main peak shows less dependence on the crystallization temperature.

Then, it can be concluded that the double melting behavior of PEEK could be related to two initial distinct crystallite populations showing two different thicknesses and/or perfection degrees. The thicker lamellae are first formed and melt at higher temperature whereas the smaller are developed later during the holding and melt at lower temperatures in agreement with the conclusions of Basset et al.<sup>16</sup> Such a result does not exclude the possible reorganization occurring on increasing the temperature, even at a high heating rate because the recording of the thermograms requires the crossing of the TTT curves, that is, the crystallization domain.

It can be stated that only one exothermic peak can be observed on DSC thermograms. But, recently Chen and Porter clearly resolved two crystallization stages through the thermal mechanical analysis of the crystallization behavior of PEEK.<sup>35</sup>

#### Origin of Two Crystallite Populations: Influence of Thermal History in Molten State

According to some studies, these two populations of crystallites originate from a segregation phenomenon of macromolecular chains occurring on

crystallization.<sup>21,22,36</sup> But for Basset,<sup>16</sup> the development of thicker lamellae which occur quickly, hindered the growth of the new crystallites because as the crystallization advances, the mobility of the surrounding amorphous material is reduced and the diffusion process is reduced.

Another interpretation for the origin of the double population of lamellae that includes the previous one, can be proposed taking into account the self nucleation phenomenon. As a matter of fact, local organization of macromolecules, "memory" of the previous crystalline order, could survive the temperatures up to the observed bulk melting temperatures.<sup>3,4,13,36,37</sup> Thus, on isothermal or nonisothermal crystallizations, these remnants of former crystals could grow rapidly and large lamellae are quickly formed. The development of the thinner or less stable lamellae is delayed because it first requires a nucleation period. Moreover, as self nuclei grow, both the amount and the molecular mobility of the surrounding crystallizable material progressively decrease. Then, the nucleation and growth of the new lamellae are deterred. In these conditions, both the number and size of these secondary crystallites can be less than those exhibited by the primary lamellae.

In order to support such an origin, implying a self-nucleation process in the double population of lamellae, the influence of the thermal history in the

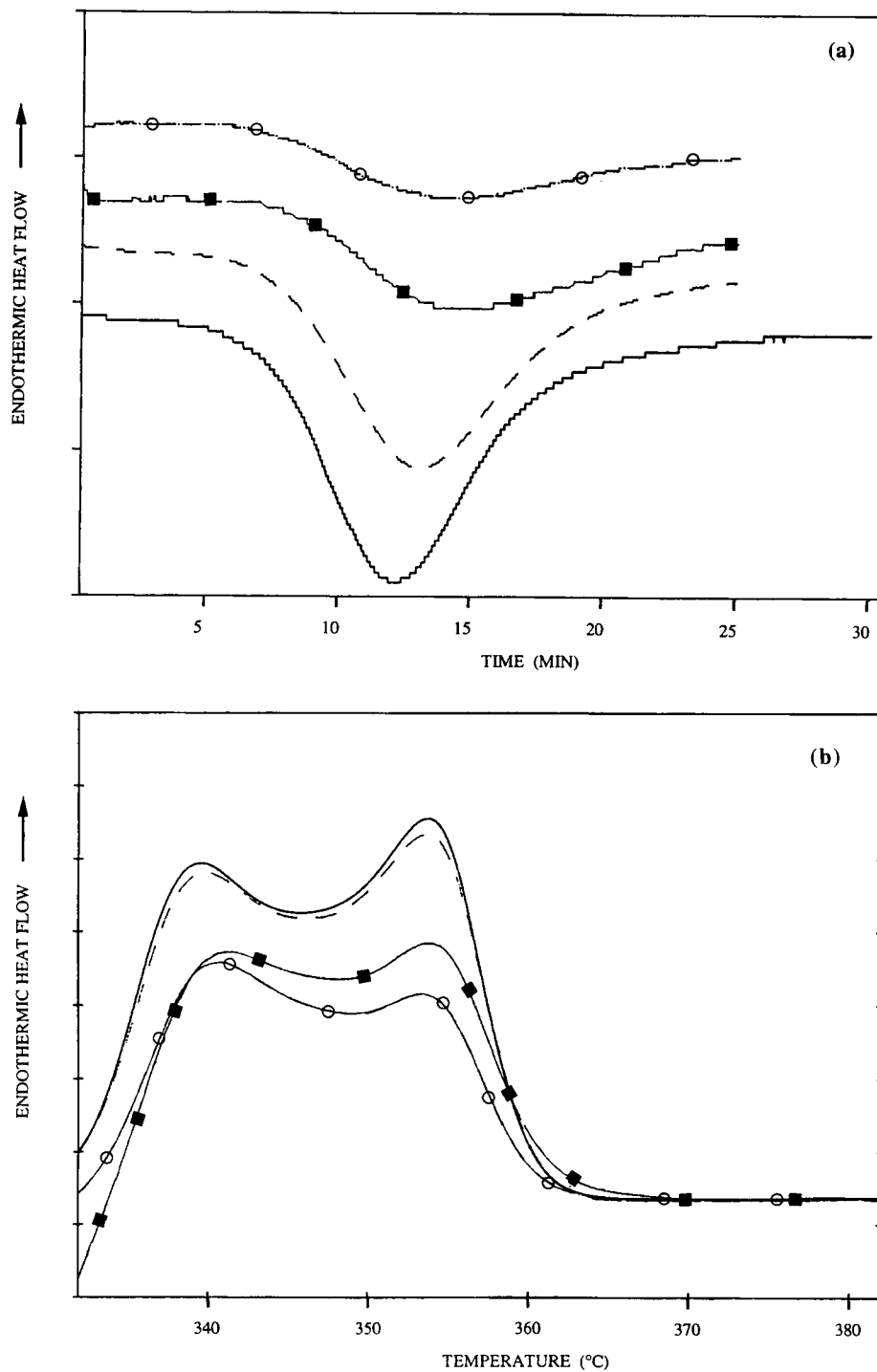


**Figure 7** (a) Crystallization exotherms recorded at 320°C for 30 min and (b) melting endotherms recorded at 100°C/min of such isothermally crystallized samples previously melt annealed at 370°C for (—) 5 min; (---) 1 h; (—■—■) 5 h; (—○—○) 12 h.

melt on the crystallization kinetics and melting behavior was analyzed.

#### DSC Analysis

Isothermal crystallization curves were recorded at 320°C for 30 min after melt annealing at 370°C,

under helium atmosphere, for various times. Such an annealing temperature is chosen because at this temperature, remnants of former crystals could survive and thermal degradation is limited.

The exothermic peak recorded by DSC at 320°C is shown in Figure 7(a). An asymmetric crystalli-



zation peak is detected for all samples whatever the melt annealing time. As the annealing time in the molten state temperature is increased, crystallization enthalpy value is reduced (Table II). Moreover, isothermal crystallization curves are found to shift to longer times as the melt annealing time is increased from 5 min to 5 h. The location of the peak crystallization time of the sample melt annealed for 12 h at 370°C exhibits a weak shift to shorter times compared to that displayed by a sample kept for 5 h at the same temperature.

Melting curves of these crystallized samples are shown in Figure 7(b). Whatever the melt annealing time, two melting peaks are observed. With increased annealing time at 370°C, the melting enthalpy value decreases (Table II). This is in agreement with the decrease in the crystallization enthalpy described above. With increasing the melt annealing time, the melting peak temperatures remain respectively unchanged. But, the pattern of the endothermic curves is modified with increasing annealing time in the molten state. As a matter of fact, for the sample melt annealed for 5 min, the magnitude of the upper temperature peak is greater than that of the lower temperature maximum. When the holding time is increased at 370°C, the relative height of the upper temperature peak becomes smaller than that of the related lower temperature peak and the global area under the endothermic curve decreases.

Thus, the three main effects induced by the increase in the melt annealing time at 370°C on isothermal crystallization and resulting melting behaviors are the following: a delay in the crystallization phenomenon; a decrease in the amount of crystallizable material; and a change in the pattern of the endothermic curves, that is, a relative decrease in the magnitude of the upper melting peak related to the melting of the thicker lamellae.

Such effects could result from the following two origins, the first of which is the progressive disappearance of the remnants of former crystals or ordered regions in the melt. As a matter of fact, with

increased holding time at 370°C in the molten state, the increase in the delay of crystallization can be interpreted as the result of a decrease in the number of self nuclei. It can be assumed that the upper endothermic peak is related to the melting of the thicker lamellae formed from the self nuclei whereas the lower endothermic peak is due to the melting of the thinner lamellae whose formation proceeds from both nucleation and growth at the crystallization temperature. In these conditions, the change in the pattern of the endothermic peak, that is the relative decrease in the magnitude of the upper temperature peak with increasing the melt annealing time, could be consistent with a decrease in the number of the self nuclei as the melt becomes more homogeneous. The decrease in the amount of crystallizable material with an increased melt annealing time at 370°C could indicate that the developed crystallinity at 320°C primarily depends on the presence of self nuclei which can grow easily.

The second origin is the progressive cross-linking and/or chain branching of the polymer melt. Such an origin must be examined because it is well-known that thermal degradation at high temperatures, even under an inert atmosphere, could modify the crystallization kinetics.<sup>3,4,14,25,38,39</sup> Thus, the decrease in both the crystallization rate and the amount of crystallization material as the reduction in the relative fraction of thicker lamellae with increasing the melt annealing time, could result from a decrease in the molecular mobility of chains induced by the cross-linking of the polymer.

#### *Cross-linking or Disappearance of Self Nuclei*

In order to give evidence for a possible thermal degradation process, IR analysis was performed on PEEK films primary melt annealed at 370°C for various annealing times, 5 min, 1 h, 5 h, and 12 h and then quenched in liquid nitrogen. To better detect the changes that occur on melt annealing treatments, the spectrum recorded for the as-received sample chosen as the reference spectrum was subtracted from the spectra of the melt annealed samples (Fig. 8).

No significant changes can be detected between the reference sample and the spectra displayed by the samples held at 370°C for 5 min and 1 h, whatever the analyzed wave number can be. Then, according to such an analysis, it can be concluded that these two thermal treatments do not induce thermal degradation in PEEK. Accordingly, it can be suggested that the increase in the delay of crystallization and the decrease in the amount of crystallizable material observed from the sample held for 1 h with

**Table II Influence of Melt Annealing Time on Crystallization and Melting Enthalpies**

Melt Annealing Time at 370°C	Enthalpies (J/g)	
	Crystallization	Melting
5 min	-37	+39
1 h	-32	+38
5 h	-17	+27
12 h	-12	+24

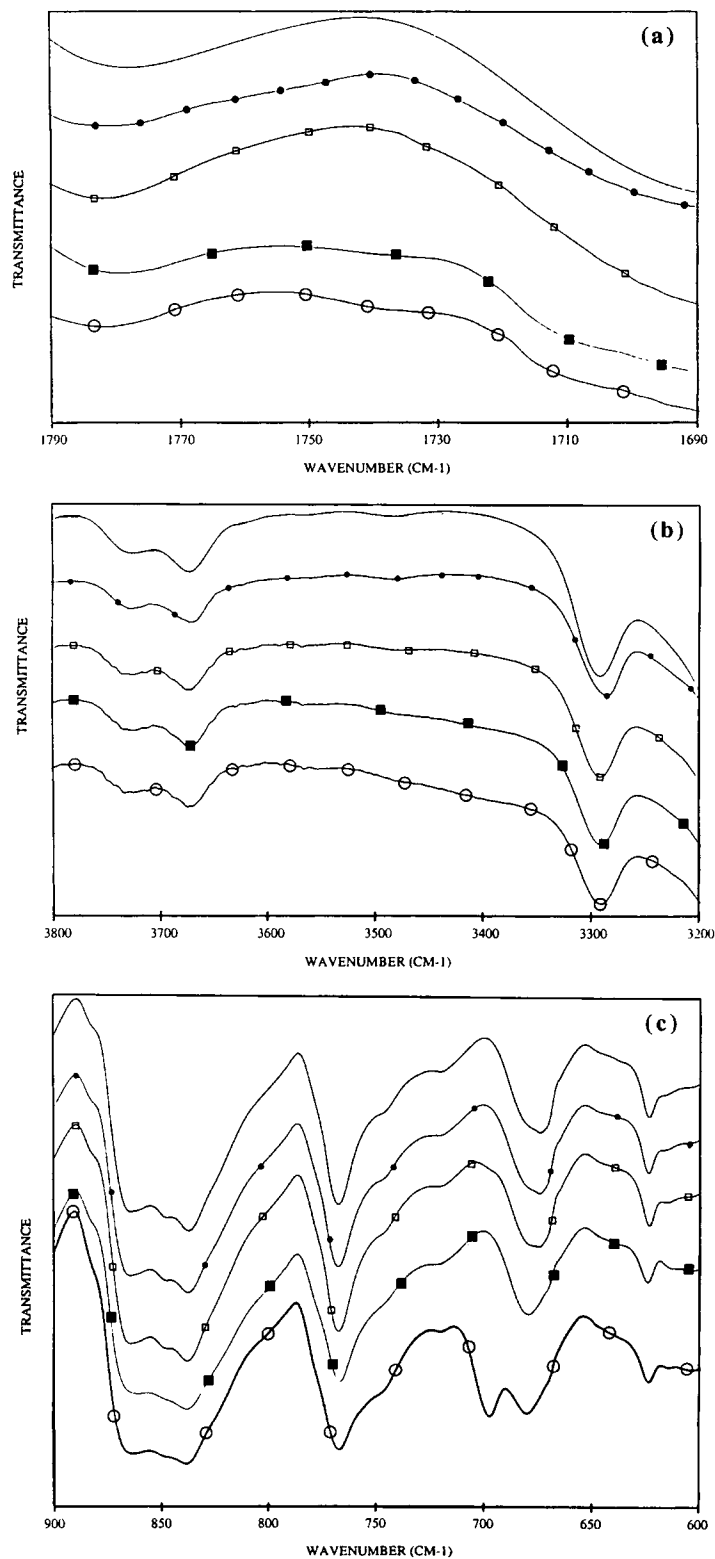


**Figure 8** Transmission IR spectra (a) in the carbonyl region and (b) in the 3200–3800  $\text{cm}^{-1}$  wave number range for PEEK films and (c) in the 900–600  $\text{cm}^{-1}$  wave number range for PEEK powder samples. The samples were melt annealed at 370°C under nitrogen gas for (—●—●—) 5 min; (—□—□—) 1 h; (—■—■—) 5 h; and (—○—○—) 12 h. The “as-received” PEEK spectrum (—) is given as the reference spectrum.

respect to the sample held for 5 min could only result from the decrease in the amount self nuclei and not from a cross-linking of the polymer.

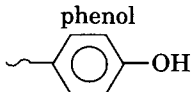
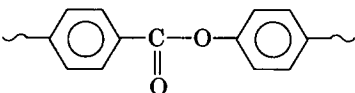
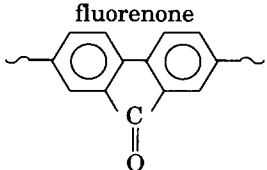
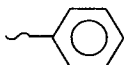
No significant changes between the patterns of the endothermic curves [Fig. 7(b)] displayed by these two samples, that is, no significant relative decrease in the magnitude of the upper temperature peak with increasing the annealing time at 370°C from 5 min to 1 h, were noted. Such a result does not exclude the hypothesis based on the presence of self nuclei that could give rise to the main upper temperature peak. Therefore, it can be noted that for the sample melt annealed for 1 h, the crystallization enthalpy is lower than the melting enthalpy (Table II). It can be concluded that reorganization has occurred on recording the endothermic curve because the TTT curves are crossed on heating from 320°C to the melting temperature range. Then the lower endothermic peak could be due not only to the melting of the secondary population of crystallites developed on isothermal conditions but also to the new crystallites formed on heating. Such a conclusion is consistent with the high nucleation ability of PEEK even at high temperatures.<sup>1,40</sup>

The patterns of the FTIR spectra recorded for the sample melt annealed for 12 h show significant changes with respect to those displayed by samples held at the same temperature for 5 min and 1 h. FTIR spectra recorded for such a sample in the

1690–1790  $\text{cm}^{-1}$  wave number range [Fig. 8(a)] show two new absorption bands located at 1710 and 1738  $\text{cm}^{-1}$ . In agreement with Cole and Casella,<sup>41</sup> these bands can be assigned to the formation of degradation products, fluorenone structures and ester groups, respectively (Table III). In the 3200 and 3800  $\text{cm}^{-1}$  wave number range, the spectrum recorded for this sample [Fig. 8(b)] shows a weak peak as a shoulder at about 3400  $\text{cm}^{-1}$ . Such an absorption band could arise from the formation of phenol groups, as previously suggested by Cole and Casella.<sup>41</sup> Moreover, spectra were recorded in the 900–600  $\text{cm}^{-1}$  wave number range of PEEK films first annealed at 370°C for various annealing times and then reduced to powder [Fig. 8(c)]. The pattern of the spectrum displayed by the sample previously melt annealed at 370°C for 12 h, is different from those recorded for the as-received specimen and melt annealed specimens for 5 min and 1 h. For the sample melt annealed for 12 h, weak modifications affect the large absorption bands at about 850 and 680  $\text{cm}^{-1}$ , respectively. But these changes could be related to the formation of multisubstituted phenylene rings. Moreover for the sample held for 12 h, a well-defined band centered at 700  $\text{cm}^{-1}$  and a band as a shoulder at about 740  $\text{cm}^{-1}$  can be observed. These bands could be assigned to the out-of-plane C—H deformation of monosubstituted phenylene rings.

On the FTIR spectra recorded for the sample melt

**Table III Chemical Functions that Could Be Formed on PEEK Degradation Process and Respective Absorption Bands**

Chemical Functions	Wave Number of New Absorption Bands and Assignment
<p>phenol</p> 	O—H stretching ( $\sim 3400 \text{ cm}^{-1}$ )
<p>ester</p> 	C=O stretching ( $\sim 1740 \text{ cm}^{-1}$ )
<p>fluorenone</p> 	C=O stretching ( $\sim 1710 \text{ cm}^{-1}$ ) Out-of-plane C—H deformation of 1,2,4 trisubstituted phenylene ring (two peaks in the 900–800 $\text{cm}^{-1}$ range)
<p>monosubstituted phenyl</p> 	Out-of-plane C—H deformation of monosubstituted phenylene ring (two peaks at $\sim 740$ and $\sim 690 \text{ cm}^{-1}$ )

annealed for 5 h at 370°C, such changes can be also detected. But the magnitude of the modifications is significantly less than those exhibited by the sample annealed for the longest time. It can also be noted that this sample does not exhibit the well-defined absorption band located at about 700 cm<sup>-1</sup>, characteristic of the formation of monosubstituted phenylene rings as the sample melt annealed for the longest time.

According to previous works,<sup>4,38</sup> the PEEK degradation occurs in two steps. The first one is a random chain scission at the ether and carbonyl linkage. In the second step, the free ether, carbonyl, and aryl thus produced can terminate by transfer abstracting hydrogen or by combination with an adjacent radical to produce cross-links. Thus, various chemical functions can be formed during such a complex degradation mechanism. According to the thermal degradation mechanism proposed by Hay and Kemmish<sup>38</sup> and the IR analysis reported by Cole and Casella,<sup>41</sup> the new absorption bands previously observed could arise from degradation products (Table III). Then, the IR spectrum modifications observed for samples melt annealed at 370°C for 12 h could be consistent with a significant PEEK thermal degradation process that includes both scission and cross-linking (and/or branching) steps. Thus, in such a sample, it appears that thermal degradation could result in a significant amount of monosubstituted phenylene rings. Such an observation could give evidence for a scission macromolecular chain mechanism. According to Hay and Kemmish,<sup>38</sup> such a degradation involves a cross-linking process. It can then be proposed that thermal degradation occurring in the sample melt annealed at 370°C for 12 h could induce a global widening in the molecular weight distribution of PEEK, that is, widening toward both the lower and higher molecular weights because of the chain scission and cross-linking processes, respectively.

Accordingly, the decrease in the crystallization ability observed from DSC experiments in this sample (12 h at 370°C) could mainly result from chemical modifications induced by thermal degradation. In particular, the significant decrease in the amount of crystallizable material observed for the 370°C, 12 h sample could be due to a decrease in molecular mobility induced by cross-linking of the polymer. The crystallite growth is then hindered. The observed decrease in the relative magnitude of the upper temperature peak is consistent with this result.

From FTIR analysis, it cannot be excluded that a possible thermal degradation occurred in the sample melt annealed for 5 h at 370°C. But the mag-

nitude of the spectrum modifications is weak. It can be noted that these spectrum changes only concern the absorption bands exhibiting strong magnitude. Moreover, such spectrum modifications are only well identified when using films of 250 μm for which the magnitude of FTIR response is the highest. Then, it can be suggested that the significant decrease in the crystallization ability observed with increasing the annealing time from 1 to 5 h could not only be due to the thermal degradation. Such a decrease in the crystallization ability and the change in the pattern of the melting endotherm observed for the longest annealing time could result from the superimposition of two phenomena, the decrease in the amount of self nuclei and cross-linking of the polymer due to thermal degradation. These phenomena act in the same way.

## CONCLUSION

The TTT diagram of PEEK was established. The "C" shape of the TTT diagram results from the nucleation phenomenon following the growth process. Such a diagram shows that the overall crystallization rate goes through a maximum in the 175–290°C temperature range. At low supercooling (above 290°C), the growth rate is faster than the nucleation rate. At these temperatures, it can be suggested that developed lamellae could be larger. At high supercooling (below 175°C), the growth rate is slower than the nucleation rate and it can be assumed that the so-developed crystallites at these temperatures could be smaller.

Samples isothermally crystallized at high or low supercooling degree exhibit two melting peaks. On increasing the annealing time at the crystallization temperature, it was observed that the upper temperature peak first rises and the lower melting peak develops later. The location of this secondary peak is shifted to the higher temperatures when increasing the annealing time at the crystallization temperature. The double melting behavior is related to a bimodal distribution in the size of lamellae developed on a two-step crystallization.

The origin of the double population of lamellae was discussed through the analysis of the influence of the thermal history on both crystallization ability and the pattern of the endothermic curves. Thus, the observed decrease in the crystallization ability of PEEK with increasing holding time in the molten state has two possible causes: the progressive disappearance of remnants of the former crystals and a progressive thermal degradation leading to a cross-

linking of the polymer. These two causes act in the same way: they hinder the crystallization kinetics.

The authors are grateful to Mr. K. D. Gilliatt and Mrs. A. Guinet (ICI film UK and France) for providing amorphous PEEK films. They thank Pr. R. Legras and Dr. A. Jonas (University of Louvain-la-Neuve) for helpful discussions. We are indebted to Mrs. A. C. Grillet for her scientific cooperation.

## REFERENCES

1. S. Kumar, P. Anderson, and W. W. Adams, *Polymer*, **27**, 329 (1986).
2. D. J. Blundell and B. N. Osborn, *Polymer*, **24**, 953 (1983).
3. Y. Deslandes, M. Day, N. F. Sabir, and T. Suprunchuk, *Polym. Compos.*, **10**, 360 (1989).
4. A. Jonas and R. Legras, *Polymer*, **32**, 2691 (1991).
5. G. S. H. Gupta and R. Salovey, *Polym. Eng. Sci.*, **30**, 453 (1990).
6. F. J. Medellin-Rodriguez and P. J. Phillips, *Polym. Eng. Sci.*, **30**, 860 (1990).
7. J. M. Chalmers, W. F. Gaskin, and M. W. Mackenzie, *Polym. Bull.*, **11**, 433 (1984).
8. A. Jonas, R. Legras, and J.-P. Issi, *Polymer*, **32**, 3364 (1991).
9. A. J. Lovinger and D. D. Davis, *Polym. Commun.*, **26**, 322 (1985).
10. C.-M. Hsiung, M. Cakmak, and J. L. White, *Polym. Eng. Sci.*, **30**, 967 (1990).
11. Y. Deslandes, F.-N. Sabir, and J. Roovers, *Polymer*, **32**, 1267 (1991).
12. M. Day, Y. Deslandes, J. Roovers, and T. Suprunchuk, *Polymer*, **32**, 1258 (1991).
13. A. Franbourg and F. Rietsch, *Polym. Bull.*, **24**, 445 (1990).
14. Y. Lee and R. S. Porter, *Macromolecules*, **21**, 2770 (1988).
15. P. Cebe and S.-D. Hong, *Polymer*, **27**, 1183 (1986).
16. D. C. Bassett, R. H. Olley, and I. A. M. Al Raheil, *Polymer*, **29**, 1745 (1988).
17. D. J. Blundell, *Polymer*, **28**, 2248 (1987).
18. S. S. Chang, *Polym. Commun.*, **29**, 138 (1988).
19. Y. Lee and R. S. Porter, *Macromolecules*, **20**, 1336 (1987).
20. Y. Lee, R. S. Porter, and J. S. Lin, *Macromolecules*, **22**, 1756 (1989).
21. S. Z. D. Cheng, M.-Y. Cao, and B. Wunderlich, *Macromolecules*, **19**, 1868 (1986).
22. M. P. Lattimer, J. K. Hoobs, M. J. Hill, and P. J. Barham, *Polymer*, **33**, 3971 (1992).
23. K. Honnecke, *Angew. Makromol. Chem.*, **198**, 15 (1992).
24. J. K. Chung and P. Cebe, *J. Polym. Sci., Polym. Phys. Ed.*, **30**, 163 (1992).
25. K. Mai, M. Zhang, H. Zeng, and S. Qi, *J. Appl. Polym. Sci.*, **51**, 57 (1994).
26. N. Alberola, *J. Mater. Sci.*, **26**, 1856 (1991).
27. B. Wunderlich, *Macromolecular Physics*, Vol. 3, Academic, New York, 1990.
28. R. Alamo and L. Mandelkern, *J. Polym. Sci., Polym. Phys. Ed.*, **24**, 2087 (1986).
29. S. Z. D. Cheng, D. P. Heberer, H.-S. Lien, and F. W. Harris, *J. Polym. Sci., Polym. Phys. Ed.*, **28**, 655 (1990).
30. P. T. Holdsworth and A. Turner-Jones, *Polymer*, **12**, 195 (1970).
31. M. Yagpharov, *J. Therm. Anal.*, **31**, 1073 (1986).
32. A. M. Freedman, D. C. Bassett, A. S. Vaughan, and R. H. Olley, *Polymer*, **24**, 1163 (1986).
33. H. Marand and A. Prasad, *Macromolecules*, **25**, 1731 (1992).
34. H. X. Nguyen and H. Ishida, *Polym. Prep.*, **26**, 273 (1985).
35. H.-L. Chen and R. S. Porter, *Polymer*, **34**, 4576 (1993).
36. J. Rault, M. Sotton, C. Rabourdin, and E. Robelin, *J. Phys.*, **41**, 1459 (1980).
37. H. X. Nguyen and H. Ishida, *Polymer*, **27**, 1400 (1986).
38. J. N. Hay and D. J. Kemmish, *Polymer*, **28**, 2047 (1987).
39. M. Day, T. Suprunchuk, J. D. Cooney, and D. M. Wiles, *J. Appl. Polym. Sci.*, **36**, 1097 (1988).
40. A. Franbourg and F. Rietsch, *Ann. Chim. Fr.*, **15**, 367 (1990).
41. K. C. Cole and I. G. Casella, *Thermochim. Acta*, **211**, 209 (1992).

Received September 30, 1993

Accepted March 13, 1994